Convergence of shock waves generated by underwater electrical explosion of cylindrical wire arrays between different boundary geometries

D. Yanuka,[1] M. Kozlov,[2] H. E. Zinowits,[1] and Ya. E. Krasik[1]
[1]*Physics Department, Technion, Haifa 32000, Israel*
[2]*Center for Energy Research, National Laboratory Astana, Nazarbayev University, Astana 010000, Republic of Kazakhstan*

(Received 6 September 2015; accepted 8 October 2015; published online 20 October 2015)

The results of experiments and numerical simulations of a shock wave propagating between either conical or parabolic bounding walls are presented. The shock wave was generated by a microsecond timescale underwater electrical explosion of a cylindrical wire array supplied by a current pulse having an amplitude of ~230 kA and a rise time of ~1 μs. It is shown that with the same energy density deposition into the exploding wire array, the shock wave converges faster between parabolic walls, and as a result, the pressure in the vicinity of convergence is ~2.3 times higher than in the case of conical walls. The results obtained are compared to those of earlier experiments [Antonov *et al.*, Appl. Phys. Lett. **102**, 124104 (2013)] with explosions of spherical wire arrays. It is shown that at a distance of ~400 μm from the implosion origin the pressure obtained in the current experiments is higher than for the case of spherical wire arrays. © *2015 AIP Publishing LLC*. [http://dx.doi.org/10.1063/1.4934217]

I. INTRODUCTION

The subject of strongly compressed hot matter is of interest for different applications as well as for basic research.[1–4] Several approaches have been used to obtain this extreme state of matter such as z-pinch, high power lasers, and heavy ion beams.[5–7] However, these approaches require large facilities and expensive experimental setups with a stored energy of $\geq 10^5$ J. Recent experiments[8–10] with setups having a moderate stored energy of $\leq 6 \times 10^3$ J showed that extreme states of matter can be obtained using either underwater electrical explosions of single wires or the converging shock waves (SWs) generated by underwater electrical explosions of cylindrical or spherical wire arrays. In the case of the explosion of single wires in water, an energy density of up to 500 eV/atom, pressure of $\sim 10^{10}$ Pa, and temperature of a few eV were achieved inside the wires.[11] In the case of converging SWs, the largest values of the pressure ($\leq 6 \times 10^{12}$ Pa), density (≤ 9 g/cm^3), and temperature (≤ 16 eV) of water in the vicinity of the implosion were calculated for a spherical wire array explosion based on SW time-of-flight (TOF) data.[10] In this approach, assuming spherical uniformity of the converging SW and self-similarity of the SW propagation in water, the value of pressure P_{SW} versus the distance from the origin, i.e., radius R_{SW}, increases as $P_{SW} \propto R_{SW}^{-1.33}$, due to the fast decrease in the SW surface as $S \propto R_{SW}^2$.

Mdivnishvili *et al.*[12] suggested that by using boundaries with a geometry that provides a faster decrease in the SW surface $S \propto R_{SW}^3$ the parameters (pressure, density, and temperature) of matter in the vicinity of the SW's convergence can be increased as compared with the case of a spherical SW implosion. Indeed, in the case of an adiabatic SW convergence, as the surface of the SW decreases faster, due to energy conservation, the energy density behind the SW front must increase faster. This leads to a higher pressure gradient and consequently to a faster propagation velocity of the SW. Self-similar analysis and calculations based on the Checter-Chisnell-Witham[13] theory showed similar results, namely, a 1.5 times larger power-law index where $S \propto R_{SW}^3$ than in a spherical implosion. In addition, the experimental studies of Mdivnishvili *et al.*[12] with planar and spherical bounding walls connected each other at the symmetry point showed that indeed the SW generated by the electrical explosion of a ring-surface discharge converges faster than one generated by a cylindrical implosion. These experiments were conducted in air at a ~20 μs timescale of the surface discharge duration, which could lead to a significant expansion of the discharge channel. The latter can be avoided in an underwater electrical explosion of wires due to the near incompressibility of water.

In recent proof of principle experiments[14] with nanosecond timescale underwater electrical explosions (storage energy of ~0.4 kJ) of planar wire arrays, it was demonstrated that a generated SW propagating between parabolic walls converges faster than one propagating between straight walls, leading to higher water parameters (density, pressure, and temperature) in the vicinity of the convergence axis. In this paper, we present the results of experiments and numerical simulations of an SW generated by the microsecond timescale underwater electrical explosion (storage energy of ~3.6 kJ) of a cylindrical wire array, propagating between either conical ($S \propto R_{SW}^2$) or parabolic ($S \propto R_{SW}^3$) bounding walls (see Fig. 1). The purpose of the research was to show that the SW converges faster between parabolic walls for the same amount of stored energy in the pulsed generator, and as a result the water parameters in the vicinity of convergence are higher than in the case of conical walls.

II. EXPERIMENTAL SETUP

A high-current generator[15] with stored energy of ~3.6 kJ generating a current pulse with an amplitude of ~300 kA and a rise time of ~1 μs was used in these

 © 2015 AIP Publishing LLC

Reuse of AIP Publishing content is subject to the terms at: https://publishing.aip.org/authors/rights-and-permissions. Downloaded to IP: 132.68.75.150 On: Sun, 17 Apr 2016 08:21:08

FIG. 1. Cylindrical wire array with two parabolic walls.

experiments. The current pulse was delivered to a 3 cm diameter cylindrical array consisting of 40–70 Cu wires 80–100 μm in diameter and 4 cm in length (see Fig. 1). Experiments were conducted with two types of stainless steel walls inserted inside the array: conical walls (Fig. 2(a)) and parabolic walls (Fig. 2(b)). The conical walls represented the geometry of SW convergence inside the segment of a sphere, and the parabolic walls allowed us to study SW convergence in a super-spherical geometry. The SW reflection coefficient for stainless steel can be estimated as $\sim$0.94, and thus, one can consider an SW convergence limited by almost rigid boundaries. The walls were fixed in holders made of Delrin, which were placed coaxially between the two electrodes serving as support for the wire array. This assemble was connected between the high-voltage (HV) and grounded electrodes located in the experimental chamber filled with distilled water. During the wire array electrical explosion, the potential difference between the walls (wall acquire floating potentials) limits the minimal distance at the axis between the walls at which water breakdown was not realized. In our experiments, it was found that a 1 mm distance satisfied this condition. The same concern is related to the height of the Delrin holders, which should be sufficient to avoid a surface breakdown between the walls and the HV and grounded electrodes. The issue of energy loss due to SW propagation in the dielectric material is addressed later. The length, diameter, and number of the wires were adjusted to obtain an aperiodic discharge in which most of the stored energy is delivered to the wires during the explosion (for elaboration on the subject of wire selection, see Ref. 14).

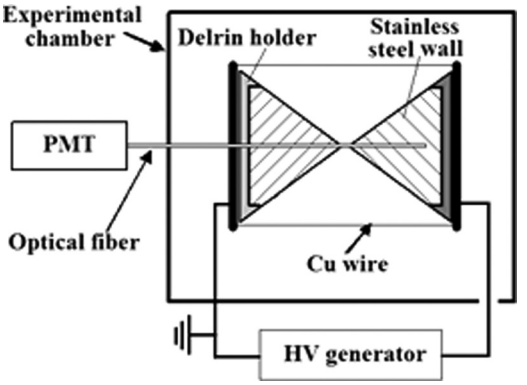

FIG. 3. Experimental setup.

The discharge current and voltage were measured using a Rogowski coil and a voltage divider, respectively. These data were used to calculate the time-dependent energy deposition into the wires. The applied high-current pulse resulted in a wire electrical explosion that generates a converging SW. To measure the TOF of the SW, an optical fiber was inserted through a hole at the center of the walls (see Fig. 3). When the SW arrived at the fiber, the strong self-emission of the fiber was recorded using a Hamamatsu photomultiplier tube (PMT). Thus, using the known time of the wires' explosion, which is characterized by a sharp decrease in the discharge current, and the time of the fiber self-emission, the TOF of the SW was calculated. The calculated energy deposition into the wires and the measured TOF of the SW, together with the equations of state (EOS) of water and copper, were then used as inputs to a 2D hydrodynamic simulation that was used to estimate the water parameters in the vicinity of the SW implosion.

III. EXPERIMENTAL RESULTS

Typical current and resistive voltage waveforms and the calculated time dependencies of the power and energy deposited into the wire array are shown in Fig. 4. To obtain the resistive voltage, the inductive voltage $L \times dI/dt$ was subtracted from the measured voltage. The discharge circuit inductance was estimated to be $L \sim 90$ nH in shots of the generator with a short-circuit load.

Typical light self-emission signals from the optical fiber that was inserted through the center of the walls for the cases of SW convergence with conical and parabolic walls can be seen in Fig. 5. Time delays between the beginning of these

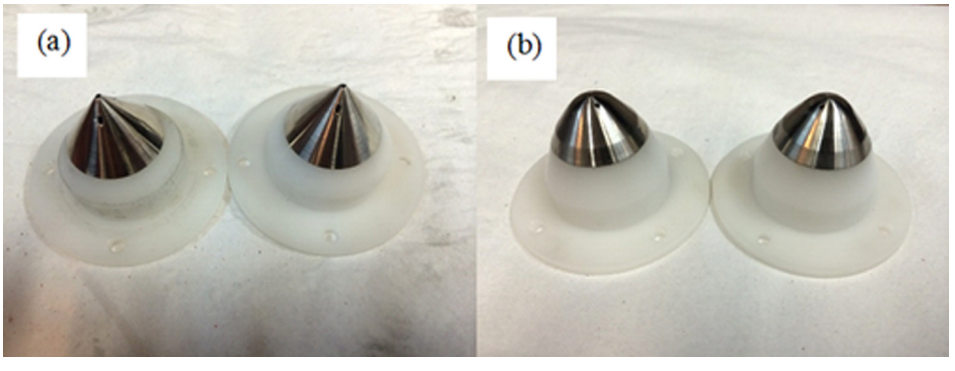

FIG. 2. (a) Conical walls. (b) Parabolic walls.

Reuse of AIP Publishing content is subject to the terms at: https://publishing.aip.org/authors/rights-and-permissions. Downloaded to IP: 132.68.75.150 On: Sun, 17 Apr 2016 08:21:08

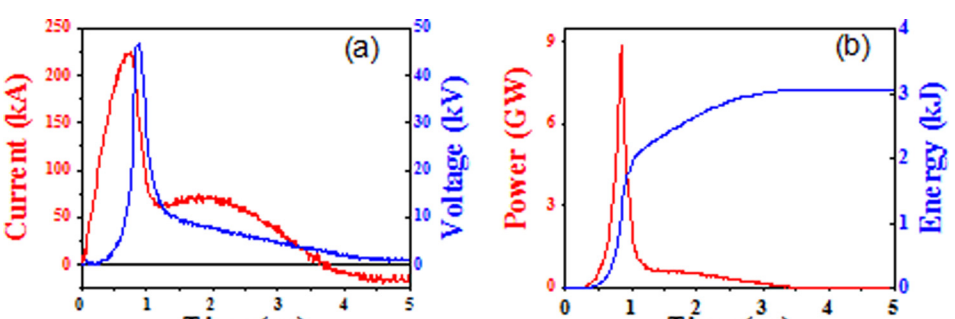

FIG. 4. (a) Waveforms of current and resistive voltage. (b) Calculated power and energy.

signals and the start of the discharge current were used for TOF measurements of the SW. Several different configurations of wire arrays (number of wires and wire diameters) were tested to find the optimal electrical explosion of the array when the most part of the preliminary stored energy is deposited into the wires during the fast decrease in the discharge current caused by the increase in the wires' resistance during the electrical explosion. For each array configuration, several explosions were carried out with conical and parabolic walls; however, no noticeable consistency in TOF data were found among the configurations. This can be explained by differences between each shot and each array. For example, there are small variations in the energy input in each shot, each array is not exactly identical, and the boundary walls slightly deform after each shot due to the strength of the SWs, and new boundaries must be manufactured. Therefore, to compare experimental and numerical simulation results, only six shots with similar current waveforms (similar peak current and rise time) were used. The TOF obtained from these shots for conical and parabolic walls was 8.52 ± 0.1 μs and 8.02 ± 0.04 μs, respectively.

IV. HYDRODYNAMIC SIMULATION

To estimate the water parameters in the vicinity of the implosion, a 2D hydrodynamic simulation was used. The code for 2D hydrodynamic simulations of SW implosion was developed in our laboratory by Kozlov, and the algorithm used is described in detail in Ref. 16. It is based on the finite volume method and uses mass, energy, and momentum conservation laws coupled with the EOS of water and copper.[17] The only input to the simulation is the energy deposition into the wires obtained from the experiment. The difference between the original simulation and the one used in this study is the symmetry of the problem, namely, in the original simulation the symmetry was along the Z axis, whereas in the present simulation the symmetry is around the X axis. Moreover, the present 2D simulation modeled the wire array as a cylindrical shell having a mass equals to the mass of the wires used in the experiment.

The simulation did not take into account the dielectric material shown in Figs. 1 and 2, because we do not have the EOS data for this material. Therefore, to simulate the energy loss due to SW dissipation in this dielectric material, water was used instead (as seen in Fig. 6), because the density of water under normal conditions (1 g/cm^3) is close to the density of Delrin (1.4 g/cm^3). Let us note here that the use of water instead of the dielectric material is compensated in some sense by the fact that the stainless steel walls used in the experiment are not completely rigid as in the simulation. The snapshots of pressure distribution obtained by hydrodynamic simulations for conical and parabolic boundaries are presented in Figs. 6(a) and 6(b), respectively, together with the axes.

The time evolution of the pressure versus time at a distance of $\sim$400 μm with respect to the axis is presented in Fig. 7. One can see that the peak pressure of 3.2 GPa and 7.2 GPa appears at 8.26 μs and 7.87 μs for conical and parabolic walls, respectively. These TOF numerical results are very similar to those obtained in the experiments, in particular, concerning the difference in TOF, which is $\sim$500 ns and $\sim$400 ns for the experimental and simulation results, respectively.

As can be seen in Fig. 7, the peak pressure is not realized abruptly, but rather it builds up gradually, in particular, in the case of conical boundaries. In the snapshots presented in Fig. 6, one can also see that the pressure in water does not increase as abruptly as one could expect in the case of the SW propagation. Namely, the propagation of the SW in

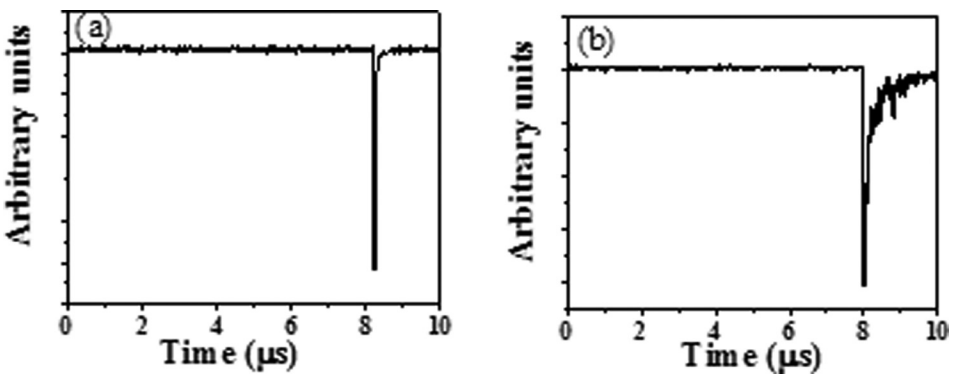

FIG. 5. Typical signals of optical fiber light emission with (a) conical walls and (b) parabolic walls.

Reuse of AIP Publishing content is subject to the terms at: https://publishing.aip.org/authors/rights-and-permissions. Downloaded to IP: 132.68.75.150 On: Sun, 17 Apr 2016 08:21:08

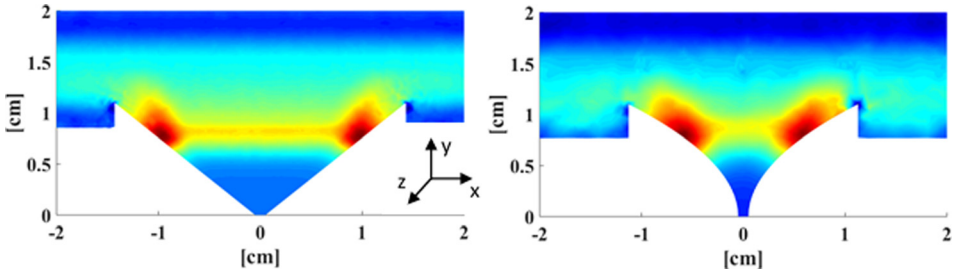

FIG. 6. Snapshots of the simulations of the SW propagation in the case of two types of bounding walls (conical and parabolic) at 5 μs from the beginning of the current pulse. The colors represent deviations from 10^5 Pa, the red being the largest deviation (~600 MPa). The black line at $r = 15$ mm was added for clarity to represent the placement of the wire array and is not a part of the snapshots.

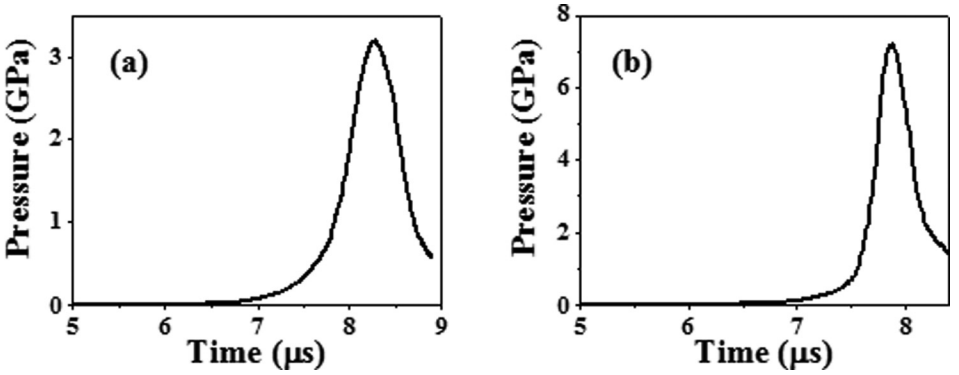

FIG. 7. Pressure at $r \sim 400$ μm for conical (a) and parabolic (b) boundaries.

water should be characterized by a rapid jump in hydrodynamic parameters (density, pressure, and temperature) behind the SW front. In the present numerical simulation, by introducing artificial viscosity, the SW front becomes smeared across 2–3 simulation cells (in physical space: ~800 μm) before it reaches the rigid boundaries. However, it then becomes smeared across 8–10 cells (in physical space: ~2 mm). The results of the simulations showed that this effect occurs because of SW reflections from the rigid boundaries. Indeed, as can be seen in Fig. 8(a), the SW front is sharp before reaching the conical boundaries. However, near the origin [see Fig. 8(b)] the SW becomes rather smeared thus preventing the efficient convergence of the SW to the origin, and therefore, decreasing the potentially high water parameters that could be obtained. Thus, it is understood that further optimization of the boundary geometry is necessary to obtain the highest value of the pressure in the vicinity of the SW implosion.

V. DISCUSSION

The experimental and numerical results indeed show that an SW propagating between parabolic walls is faster than one propagating between conical walls, resulting in a ~2.3 times larger pressure in the vicinity of the implosion. In addition, we compared these results to those obtained in experiments with a spherical array implosion recently conducted in our laboratory.[10] The TOF data for the SW generated by underwater electrical explosion of spherical arrays having 20 mm, 30 mm, and 40 mm diameters were ~4 μs, ~6 μs, and ~9.5 μs, respectively. To compare these TOF data with the data obtained in the present experiments with cylindrical wire array explosions having conical wall boundaries, a sphere with the same surface area as the cylindrical shell should be considered in order to keep the same energy density deposition. For the 30 mm cylindrical shell with a 40 mm length, the sphere diameter should be ~35 mm. The obtained TOF of the SW converging between conical walls is ~8 μs. This value is between the ~6 μs and ~9.5 μs of the SW TOF obtained in the cases of explosions using the 30 mm and 40 mm diameter spherical wire arrays, showing satisfactory agreement. In addition, using the results presented in Ref. 10 and the self-similarity relation for the pressure behind the SW front given in the introduction, one obtains that the pressure at $r \sim 400$ μm for the spherical array explosions is $P \sim 4.1$ GPa and $P \sim 7.5$ GPa for 40 mm and

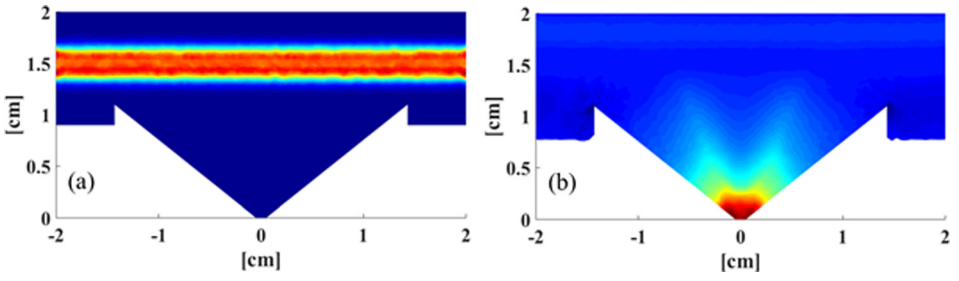

FIG. 8. Snapshots of the simulations of the SW propagation in the case of conical bounding walls at different times with respect to the beginning of the current pulse. (a) At 1.5 μs. (b) At 8 μs.

Reuse of AIP Publishing content is subject to the terms at: https://publishing.aip.org/authors/rights-and-permissions. Downloaded to IP: 132.68.75.150 On: Sun, 17 Apr 2016 08:21:08

30 mm diameter arrays, respectively. Thus, again considering the value of the pressure for a 35 mm diameter array to be ~5.8 GPa, one obtains that this exceeds the value obtained in the present experiment for conical walls, but is below the value for parabolic walls.

The value of the pressure was calculated at $r \sim 400\,\mu$m, because the results of simulations show that at smaller radii of convergence the peak pressure does not increase significantly, as opposed to the case of the spherical implosion simulation. An analysis showed that this occurs because of two competing processes governing the convergence of the SW in the present experiments, namely, the rapid increase in SW energy density due to a decrease in the SW front area versus backward reflections from the rigid boundaries (see Figs. 6 and 8).

V. SUMMARY

We showed both experimentally and by numerical calculations that an SW generated by an underwater electrical explosion of a cylindrical wire array propagates faster between parabolic walls inserted inside the array than between conical walls. Hydrodynamic calculations showed that the peak pressure obtained in the case of parabolic walls is larger than in the case of conical walls, as well as in the case of a spherical wire array explosion with the same energy density deposition into the wires. Additional research will be conducted to find the optimal geometry that minimizes the backward reflections of the SW from the boundaries resulting in higher values of pressure and temperature in the vicinity of the SW implosion.

[1]T. Ma, P. K. Patel, N. Izumi, P. T. Springer, M. H. Key, L. J. Atherton, L. R. Benedetti, D. K. Bradley, D. A. Callahan, P. M. Celliers, C. J. Cerjan, D. S. Clark, E. L. Dewald, S. N. Dixit, T. Doppner, D. H. Edgell, R. Epstein, S. Glenn, G. Grim, S. W. Haan, B. A. Hammel, D. Hicks, W. W. Hsing, O. S. Jones, S. F. Khan, J. D. Kilkenny, J. L. Kline, G. A. Kyrala, O. L. Landen, S. Le Pape, B. J. MacGowan, A. J. Mackinnon, A. G. MacPhee, N. B. Meezan, J. D. Moody, A. Pak, T. Parham, H. S. Park, J. E. Ralph, S. P. Regan, B. A. Remington, H. F. Robey, J. S. Ross, B. K. Spears, V. Smalyuk, L. J. Suter, R. Tommasini, R. P. Town, S. V. Weber, J. D. Lindl, M. J. Edwards, S. H. Glenzer, and E. I. Moses, Phys. Rev. Lett. **111**, 085004 (2013).
[2]K. K. Reeves and L. Golub, Astrophys. J., Lett. **727**, L52 (2011).
[3]J. J. Rocca, V. Shlyaptsev, F. G. Tomasel, O. D. Cortazar, D. Hartshorn, and J. L. A. Chilla, Phys. Rev. Lett. **73**, 2192 (1994).
[4]R. P. Drake, Phys. Plasmas **16**, 055501 (2009).
[5]I. M. Hall, T. Durmaz, R. C. Mancini, J. E. Bailey, G. A. Rochau, I. E. Golovkin, and J. J. MacFarlane, Phys. Plasmas **21**, 031203 (2014).
[6]B. A. Remington, R. P. Drake, and D. D. Ryutov, Rev. Mod. Phys. **78**, 755 (2006).
[7]N. A. Tahir, D. H. H. Hoffmann, A. Kozyreva, A. Shutov, J. A. Maruhn, U. Neuner, A. Tauschwitz, P. Spiller, and R. Bock, Phys. Rev. E **61**, 1975 (2000).
[8]D. Sheftman, D. Shafer, S. Efimov, K. Gruzinsky, S. Gleizer, and Ya. E. Krasik, Rev. Sci. Instrum. **83**, 103505 (2012).
[9]A. Fedotov-Gefen, S. Efimov, L. Gilburd, G. Bazalitski, V. Tz. Gurovich, and Ya. E. Krasik, Phys. Plasmas **18**, 062701 (2011).
[10]O. Antonov, S. Efimov, D. Yanuka, M. Kozlov, V. Tz. Gurovich, and Ya. E. Krasik, Appl. Phys. Lett. **102**, 124104 (2013).
[11]A. Grinenko, S. Efimov, A. Fedotov, and Ya. E. Krasik, Phys. Plasmas **13**, 052703 (2006).
[12]M. O. Mdivnishvili, I. V. Sokolov, M. I. Taktakishvili, and P. A. Voinovich, Shock Waves **9**, 149–158 (1999).
[13]G. B. Whitham, *Linear and Nonlinear Waves* (Wiley, New York, 1974).
[14]D. Yanuka, D. Shafer, and Ya. Krasik, J. Appl. Phys. **117**, 163305 (2015).
[15]S. Efimov, A. Fedotov, S. Gleizer, V. Tz. Gurovich, G. Bazalitski, and Ya. E. Krasik, Phys. Plasmas **15**, 112703 (2008).
[16]M. Kozlov, V. Tz. Gurovich, and Ya. E. Krasik, Phys. Plasmas **20**, 112701 (2013).
[17]See National Technical Information Service Document No. DE85014241 (S. P. Lyon and J. D. Johnson, Sesame: The Los Alamos National Laboratory Equation-of-State Database, LANL Rep. LA UR-92-3407, 1992). Copies may be ordered from the National Technical Information Service, Springfield, VA, 22161.

Reuse of AIP Publishing content is subject to the terms at: https://publishing.aip.org/authors/rights-and-permissions. Downloaded to IP: 132.68.75.150 On: Sun, 17 Apr 2016 08:21:08